



Falkland Islands Fisheries Department

Falkland calamari Stock Assessment, First Season 2016

Andreas Winter

May 2016

Index

Summary	3
Introduction.....	3
Methods.....	4
Stock assessment.....	8
Data.....	8
Group arrivals / depletion criteria.....	9
Depletion analyses	12
North.....	12
South.....	13
Escapement biomass.....	14
Immigration	16
Size ranges	16
Bycatch	18
References.....	20
Appendix.....	22
Falkland calamari individual weights.....	22
Prior estimates and CV	23
Depletion model estimates and CV	24
Combined Bayesian models	25

Summary

- 1) The 2016 first season Falkland calamari fishery (C license) was open from February 24th, and closed as scheduled on April 28th. A sub-area of the Loligo Box was closed from April 7th to the end of the season to conserve small (younger) calamari, west of 57°15' W and between 51°00' and 51°30' N.
- 2) 22,616 tonnes of calamari catch were reported in the C-license fishery; giving an average CPUE of 22.17 tonnes vessel-day⁻¹. Throughout the season 49.0% of calamari catch and 48.7% of fishing effort were taken north of 52° S; vs. 51.0% of calamari catch and 51.3% of fishing effort taken south of 52° S. These are the most even north / south catch and effort partitions of any recent 1st season, with higher concentration towards the centre of the Loligo Box than usual.
- 3) Sub-areas north and south of 52°S were depletion-modelled separately. In the north sub-area, seven depletion periods / immigrations were inferred to have started on March 2nd, March 5th, March 21st, March 28th, April 4th, April 11th, and April 17th. In the south sub-area, five depletion periods / immigrations were inferred to have started on February 24th, March 10th, March 25th, March 30th, and April 4th.
- 4) Approximately 43,874 tonnes of calamari (95% confidence interval: [38,489 to 82,768] tonnes) were estimated to have immigrated into the Loligo Box during 1st season 2016, of which 13,290 t north of 52° S and 30,584 t south of 52° S.
- 5) The biomass estimate for calamari remaining in the Loligo Box at the end of 1st season 2016 was:
Maximum likelihood of 24,868 tonnes, with a 95% confidence interval of [20,723 to 61,272] tonnes. With the bulk of calamari biomass entering the fishing zone as late immigrations, this season was unusual in having higher estimated calamari abundance at the end of the season than at the beginning of the season.
The risk of calamari escapement biomass at the end of the season being less than 10,000 tonnes was estimated at effectively zero.

Introduction

The first season of the 2016 Falkland calamari fishery (*Doryteuthis gahi* – Patagonian longfin squid – colloquially *Loligo*) opened on February 24th with 16 C-licensed vessels participating; none having taken the flex option to start later. Early in March one vessel suffered mechanical failure and was towed to port by a sister ship. The tow vessel and damaged vessel were allocated extensions of 2 and 3 days respectively at the end of the season for time missed from the fishery, equivalent to the flex option. A different vessel suffered mechanical failure in late March and was replaced by a sister ship for 14 days from March to early April. On April 7th, a sub-area of the Loligo Box was excluded until the end of the season to conserve small (younger) calamari, consisting of grid XNAN in its entirety and grids XNAP and XPAP west of 57°15' W. The first season ended by directed closure on April 28th, plus respectively on April 30th and May 1st for the two flex-allocated vessels.

Total reported Falkland calamari catch under first season C license was 22,616 tonnes, corresponding to a CPUE of $22616 / 1020 = 22.17$ tonnes vessel-day⁻¹ (Table 1). This CPUE was the lowest in a first season since 2011, and the lowest in a first season not closed by emergency order since 2009.

As in previous seasons, the Falkland calamari stock assessment was conducted with depletion time-series models (Agnew et al., 1998; Roa-Ureta and Arkhipkin,

2007; Arkhipkin et al., 2008). Because calamari has an annual life cycle (Patterson, 1988), stock cannot be derived from a standing biomass carried over from prior years (Rosenberg et al., 1990). The depletion model instead calculates an estimate of population abundance over time by evaluating what levels of abundance and catchability must be extant to sustain the observed rate of catch. Depletion modelling is used both in-season and for the post-season summary, with the objective of maintaining an escapement biomass of 10,000 tonnes calamari at the end of each season as a conservation threshold (Agnew et al., 2002; Barton, 2002).

Table 1. Falkland calamari season comparisons since 2004. Days: total number of calendar days open to licensed calamari fishing including (since 1st season 2013) optional extension days; V-Days: aggregate number of licensed calamari fishing days reported by all vessels for the season.

	Season 1			Season 2		
	Catch (t)	Days	V-Days	Catch (t)	Days	V-Days
2004				17,559	78	1271
2005	24,605	45	576	29,659	78	1210
2006	19,056	50	704	23,238	53	883
2007	17,229	50	680	24,171	63	1063
2008	24,752	51	780	26,996	78	1189
2009	12,764	50	773	17,836	59	923
2010	28,754	50	765	36,993	78	1169
2011	15,271	50	771	18,725	70	1099
2012	34,767	51	770	35,026	78	1095
2013	19,908	53	782	19,614	78	1195
2014	28,119	59	872	19,630	71	1099
2015	19,383*	57*	871*	10,190	42	665
2016	22,616	68	1020			

* Does not include C-license catch or effort after the C-license target for that season was switched from calamari to *Illex*.

Methods

The depletion model formulated for the Falkland calamari stock is based on the equivalence:

$$C_{\text{day}} = q \times E_{\text{day}} \times N_{\text{day}} \times e^{-M/2} \quad (1)$$

where q is the catchability coefficient, M is the natural mortality rate (considered constant at 0.0133 day^{-1} ; Roa-Ureta and Arkhipkin, 2007), and C_{day} , E_{day} , N_{day} are catch (numbers of calamari), fishing effort (numbers of vessels), and abundance (numbers of calamari) per day. In its basic form (DeLury, 1947) the depletion model assumes a closed population in a fixed area for the duration of the assessment. However, the assumption of a closed population is imperfectly met in the Falkland Islands fishery, where stock analyses have often shown that calamari groups arrive in successive waves after the start of the season (Roa-Ureta, 2012; Winter and Arkhipkin, 2015). Arrivals of successive groups are inferred from discontinuities in the catch data. Fishing on a single, closed cohort would be expected to yield gradually decreasing CPUE, but gradually increasing average individual sizes, as the squid

grow. When instead these data change suddenly, or in contrast to expectation, the immigration of a new group to the population is indicated (Winter and Arkhipkin 2015).

In the event of a new group arrival, the depletion calculation must be modified to account for this influx. This was done using a simultaneous algorithm (Roa-Ureta, 2012) that adds new arrivals on top of the stock previously present, and posits a common catchability coefficient for the entire depletion time-series. If two depletions are included in the same model (i.e., the stock present from the start plus a new group arrival), then:

$$C_{\text{day}} = q \times E_{\text{day}} \times (N1_{\text{day}} + (N2_{\text{day}} \times i2_{|0}^1)) \times e^{-M/2} \quad (2)$$

where $i2$ is a dummy variable taking the values 0 or 1 if ‘day’ is before or after the start day of the second depletion. For more than two depletions, $N3_{\text{day}}$, $i3$, $N4_{\text{day}}$, $i4$, etc., would be included following the same pattern.

The Falkland calamari stock assessment was calculated in a Bayesian framework (Punt and Hilborn, 1997), whereby results of the season depletion model are conditioned by prior information on the stock; in this case the information from the pre-season survey. The season depletion likelihood function was calculated as the difference between actual catch numbers reported and catch numbers predicted from the model (equation 2), statistically corrected by a factor relating to the number of days of the depletion period (Roa-Ureta, 2012):

$$((n\text{Days} - 2) / 2) \times \log \left(\sum_{\text{days}} \left(\log(\text{predicted } C_{\text{day}}) - \log(\text{actual } C_{\text{day}}) \right)^2 \right) \quad (3)$$

The survey prior likelihood function was calculated as the normal distribution of the difference between catchability (q) derived from the survey abundance estimate, and catchability derived from the season depletion model:

$$\frac{1}{\sqrt{2\pi \cdot \text{SD}_{q \text{ survey}}^2}} \times \exp \left(- \frac{(q_{\text{model}} - q_{\text{survey}})^2}{2 \cdot \text{SD}_{q \text{ survey}}^2} \right) \quad (4)$$

Catchability q , rather than abundance N , was used for calculating the survey prior likelihood because catchability informs the entire season time series; whereas N from the survey only informs the first season depletion period – subsequent immigrations and depletions are independent of the abundance that was present during the survey.

Bayesian optimization of the depletion was calculated by jointly minimizing equations 3 and 4, using the Nelder-Mead algorithm in R programming package ‘optimx’ (Nash and Varadhan, 2011). Relative weights in the joint optimization were assigned to equations 3 and 4 as the converse of their coefficients of variation (CV), i.e., the CV of the prior became the weight of the depletion model and the CV of the depletion model became the weight of the prior. Calculations of the CVs are described in the Appendix. Because a complex model with multiple depletions may converge on a local rather than a global minimum, the optimization was stabilized by running a feed-back loop that set the q and N parameter outputs of the Bayesian joint optimization back into the in-season-only minimization (equation 3), re-calculated this minimization and the CV resulting from it, then re-calculated the Bayesian joint

optimization, and continued this process until both the in-season minimization and the joint optimization remained unchanged.

With C_{day} , E_{day} and M being fixed parameters, the optimization of equation 2 using 3 and 4 produces estimates of q and N_1 , N_2 , ..., etc. Numbers of calamari on the final day (or any other day) of a time series are then calculated as the numbers N of the depletion start days discounted for natural mortality during the intervening period, and subtracting cumulative catch also discounted for natural mortality (CNMD). Taking for example a two-depletion period:

$$N_{\text{final day}} = N_1_{\text{start day 1}} \times e^{-M(\text{final day} - \text{start day 1})} + N_2_{\text{start day 2}} \times e^{-M(\text{final day} - \text{start day 2})} - \text{CNMD}_{\text{final day}} \quad (5)$$

where

$$\begin{aligned} \text{CNMD}_{\text{day 1}} &= 0 \\ \text{CNMD}_{\text{day x}} &= \text{CNMD}_{\text{day x-1}} \times e^{-M} + C_{\text{day x-1}} \times e^{-M/2} \end{aligned} \quad (6)$$

$N_{\text{final day}}$ is then multiplied by the average individual weight of calamari on the final day to give biomass. Daily average individual weight is obtained from length / weight conversion of mantle lengths measured in-season by observers, and also derived from in-season commercial data as the proportion of product weight that vessels reported per market size category. Observer mantle lengths are scientifically precise, but restricted to 1-2 vessels at any one time that may or may not be representative of the entire fleet. Commercially proportioned mantle lengths are relatively less precise, but cover the entire fishing fleet. Therefore, both sources of data are used. Daily average individual weights are calculated by averaging observer size samples and commercial size categories where observer data are available, otherwise only commercial size categories. To smooth fluctuations, $N_{\text{final day}}$ (or N on any other day of interest) is multiplied by the expected value of the average individual weight from its GAM trend (see Appendix), rather than by the empirical value on each day.

Distributions of the likelihood estimates from joint optimization (i.e., measures of their statistical uncertainty) were computed using a Markov Chain Monte Carlo (MCMC) (Gelman and Lopes, 2006), a method that is commonly employed for fisheries assessments (Magnusson et al., 2013). MCMC is an iterative process which generates random stepwise changes to the proposed outcome of a model (in this case, the q and N of calamari) and at each step, accepts or nullifies the change with a probability equivalent to how well the change fits the model parameters compared to the previous step. The resulting sequence of accepted or nullified changes (i.e., the ‘chain’) approximates the likelihood distribution of the model outcome. The MCMC of the depletion models were run for 200,000 iterations; the first 1000 iterations were discarded as burn-in sections (initial phases over which the algorithm stabilizes); and the chains were thinned by a factor equivalent to the maximum of either 5 or the inverse of the acceptance rate (e.g., if the acceptance rate was 12.5%, then every 8th (0.125^{-1}) iteration was retained) to reduce serial correlation. For each model three chains were run; one chain initiated with the parameter values obtained from the joint optimization of equations 3 and 4, one chain initiated with these parameters $\times 2$, and one chain initiated with these parameters $\times 1/4$. Convergence of the three chains was accepted if the variance among chains was less than 10% higher than the variance within chains (Brooks and Gelman, 1998). When convergence was satisfied the three chains were combined as one final set. Equations

5, 6, and the multiplication by average individual weight were applied to the CNMD and each iteration of N values in the final set, and the biomass outcomes from these calculations represent the distribution of the estimate. The peaks of the MCMC histograms were compared to the empirical optimizations of the N values.

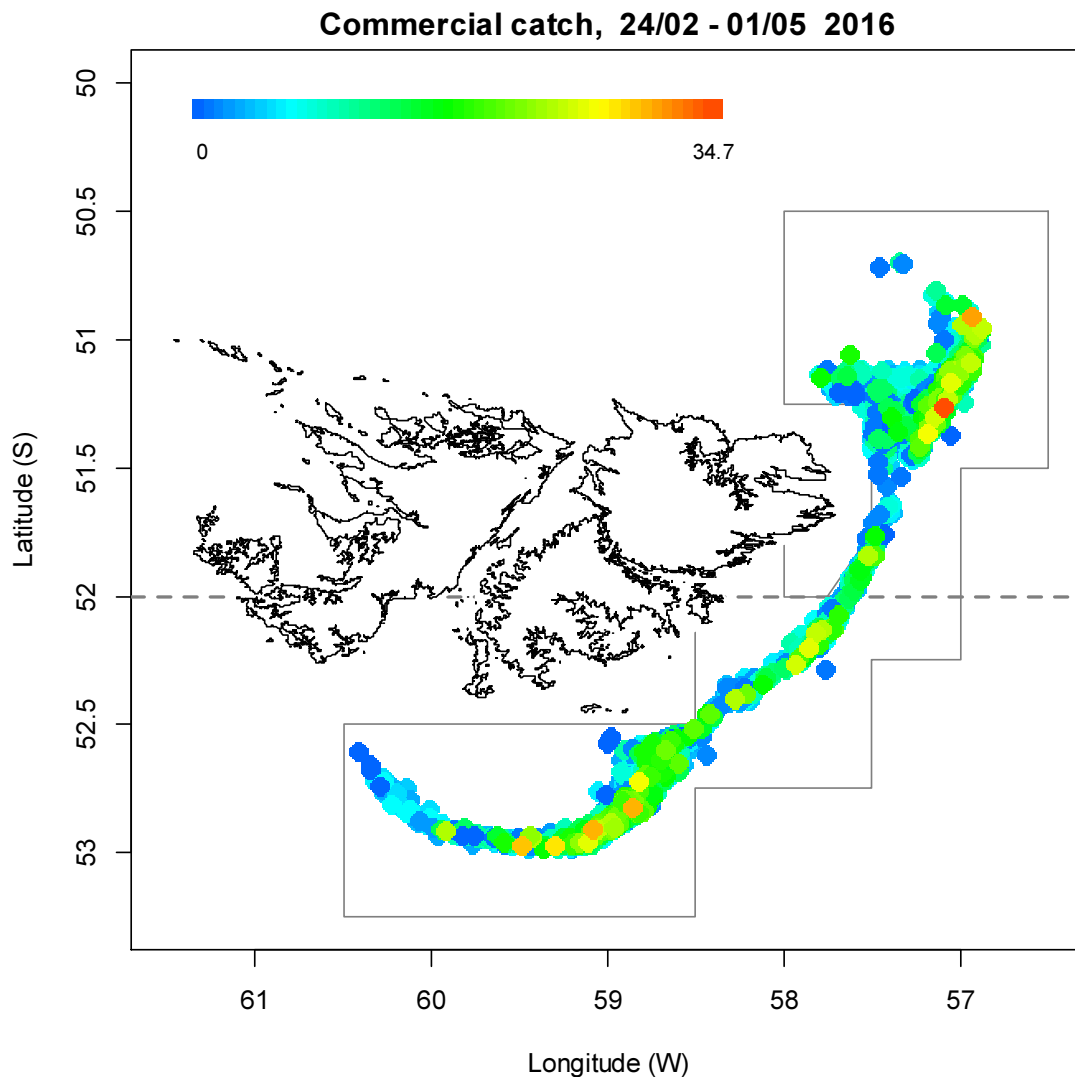


Figure 1. Spatial distribution of Falkland calamari 1st-season 2016 commercial catches, colour-scaled to catch weight (maximum = 34.7 tonnes). 3143 trawl catches were taken during the season. The Loligo Box fishing zone, as well as the 52 °S parallel delineating the boundary between north and south assessment sub-areas, are shown in grey.

Total escapement biomass is defined as the aggregate biomass of calamari on the last day of the season for north and south sub-areas combined. Calamari sub-stocks emigrate from different spawning grounds and remain to an extent segregated (Arkhipkin and Middleton, 2002). However, north and south biomasses are not assumed to be uncorrelated (Shaw et al., 2004), and therefore north and south likelihood distributions were added semi-randomly in proportion to the strength of their day-to-day correlation (semi-randomization algorithm in Winter, 2014b).

Stock assessment Data

Falkland calamari catches were characterized in this season by an uncommonly even concentration throughout the Loligo Box (Figure 1). 7.3% of the catch by weight and 11.8% of vessel-days were taken in what was previously defined as the centre sub-area, between 52° S and 52.5° S (Payá, 2009; Roa-Ureta and Arkhipkin, 2007). By comparison, in first seasons of 2011, 2012, 2013, 2014, and 2015, percentages of catch taken in the centre were 0.8%, 2.4%, 0.07%, 0.05%, and 0.8%; percentages of vessel-days taken in the centre were 2.5%, 5.5%, 1.2%, 0.6%, and 5.9% (Winter, 2011; 2012; 2013; 2014a; 2015).

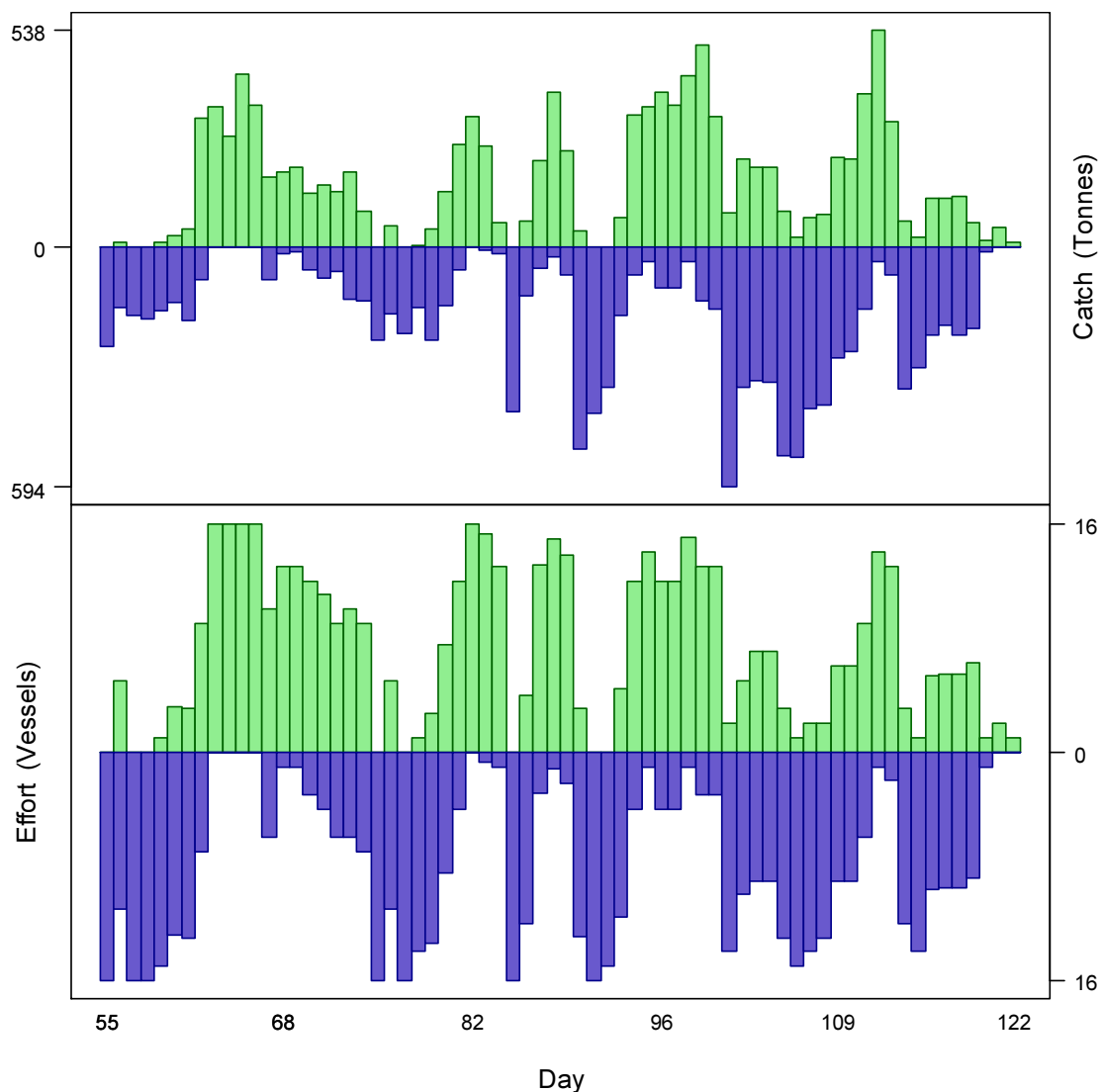


Figure 2. Daily total Falkland calamari catch and effort distribution by assessment sub-area north (green) and south (purple) of the 52° S parallel during 1st season 2016. The season was open from February 24th (chronological day 55) to April 28th (chronological day 119), plus flex days for two vessels until day 121 and for one vessel until day 122. As many as 16 vessels fished per day north of 52° S; as many as 16 vessels fished per day south of 52° S. As much as 538 tonnes calamari was caught per day north of 52° S; as much as 594 tonnes calamari was caught per day south of 52° S.

A total of 1020 vessel-days were fished during the season, with a median of 16 and no fewer than 14 vessels per day (except for the flex extensions). Vessels reported daily catch totals to the FIFD and electronic logbook data that included trawl start and end times, trawl positions, and product weight by market size categories. Two FIFD observers were deployed on three vessels in the fishery for a total of 72 observer-days (Bradley, 2016a; 2016b; Iriarte, 2016). Throughout the 68 days of the season, 4 days had no observer covering (3 of which were the extension days at the end), 56 days had 1 observer covering, and 8 days had two observers covering. Observers sampled an average of 417.3 calamari daily, and reported calamari maturity stages, sex, and mantle lengths to 0.5 cm. The length-weight relationship for converting both observer length data and commercially proportioned length data was taken from the pre-season survey (Winter et al, 2016):

$$\text{weight (kg)} = 0.112 \times \text{length (cm)}^{2.374} / 1000 \quad (7)$$

Group arrivals / depletion criteria

Start days of depletions - following arrivals of new calamari groups - were judged primarily with reference to daily changes in CPUE, with additional information from sex proportions, maturity, and average individual calamari sizes. CPUE was calculated as metric tonnes of calamari caught per vessel per day. Days were used rather than trawl hours as the basic unit of effort. Commercial vessels do not trawl standardized duration hours, but rather durations that best suit their daily processing requirements. An effort index of days is therefore more consistent.

Seven days in the north and five days in the south were identified that represented the onset of separate immigrations / depletions in the season. This exceptionally high number of immigrations (e.g., Winter and Arkhipkin, 2015) concurred with the outcome that catches and overall CPUE continued to increase in the fishery until three weeks before the end of the season (Figure 2), suggesting a generally late start to the out-migration.

- The first depletion north was identified on day 62 (March 2nd), one week after the start of the season but the first day that more than a third of the fleet fished north. Day 62 had the highest CPUE in the north until day 99 (April 8th) (Figure 3).
- The second depletion north was identified just three days later on day 65 (March 5th) with a rebound of CPUE after two days' decrease (Figure 3) and local minimal values of commercial and observer average weights, proportion of females, and average maturities (Figure 4).
- The third depletion north was identified on day 81 (March 21st) with a modest CPUE increase (Figure 3) but clear minima in commercial and observer average weights (Figure 4A & B).
- The fourth depletion north was identified on day 88 (March 28th) with a local CPUE peak (Figure 3) and one day after minima in average weights and proportion of females (Figure 4A, B & C).
- The fifth depletion north was identified on day 95 (April 4th) with steep minima in observer average weights and proportion of females (Figure 4B & C).
- The sixth depletion north was identified on day 102 (April 11th) with the highest CPUE north of the season (Figure 3), and minima in observer average weights and proportion of females (Figure 4B & C).

- The seventh depletion north was identified on day 108 (April 17th) with a local peak in CPUE (albeit taken by only two vessels, Figure 3), and the lowest minimum in commercial average weights until the end of the season (Figure 4A).
- The first depletion south was identified on day 55 (February 24th – the start of the commercial season) with 16 vessels starting the fishery in the south (Figure 2) and the highest CPUE in the south until day 70 (March 10th) (Figure 3).
- The second depletion south was identified on day 70. Besides the local CPUE peak that day (Figure 3), average weights had been at a local minimum the day before (Figure 4A & B).
- The third depletion south was identified on day 85 (March 25th) with the highest CPUE in the south up to that date (Figure 3). Average weights and maturity were not clearly associated with any time series minima (Figure 4A, B & D), resulting in this depletion start being questionable. However, the depletion model would have been difficult to execute without inferring a depletion start on this date.
- The fourth depletion south was identified on day 90 (March 30th). CPUE attained another season high (Figure 3), while average observer weight was near a local minimum (Figure 4B).
- The fifth depletion south was identified on day 95 (April 4th), when CPUE attained the second-highest peak of the season (Figure 3) and commercial average weight was at a steep local minimum (Figure 4A).

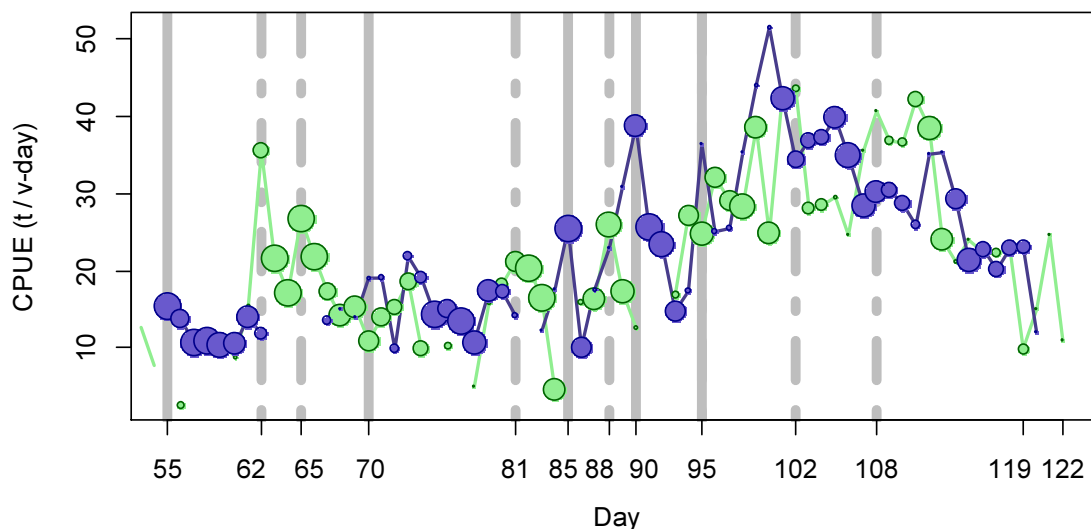
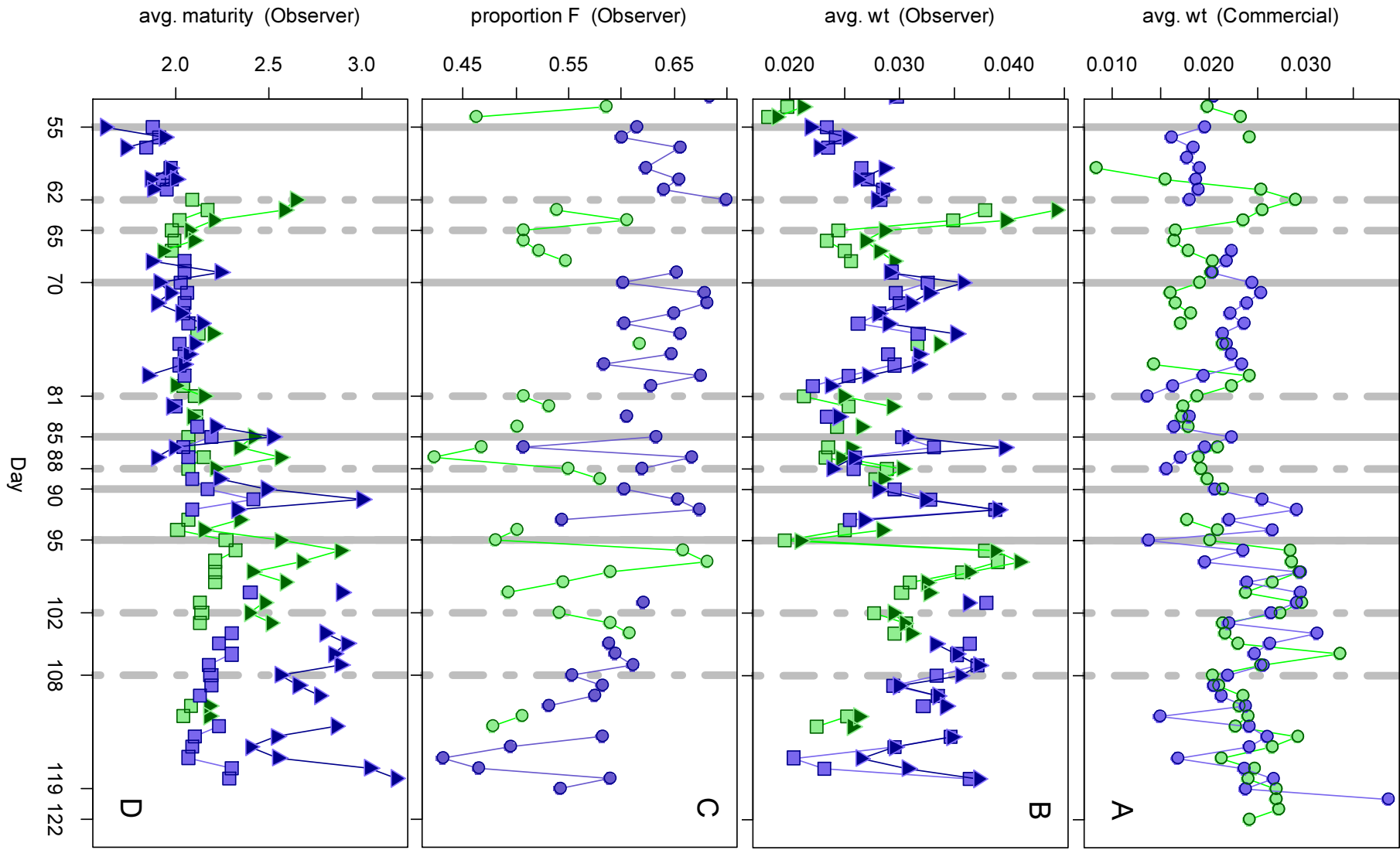


Figure 3. CPUE in metric tonnes per vessel per day, by assessment sub-area north (green) and south (purple) of 52° S latitude. Circle sizes are proportioned to the numbers of vessel fishing. Data from consecutive days are joined by line segments. Broken grey bars indicate the starts of in-season depletions north. Solid grey bars indicate the starts of in-season depletions south (day 95 was a depletion start both north and south).

Figure 4 [next page]. A: Average individual calamari weights (kg) per day from commercial size categories. B: Average individual calamari weights (kg) by sex per day from observer sampling. C: Proportions of female calamari per day from observer sampling. D: Average maturity value by sex per day from observer sampling. In all graphs – Males: triangles, females: squares, unsexed: circles. North sub-area: green, south sub-area: purple. Data from consecutive days are joined by line segments. Broken grey bars indicate the starts of in-season depletions north. Solid grey bars indicate the starts of in-season depletions south (day 95 was a depletion start both north and south).



Depletion analyses North

In the north sub-area, Bayesian optimization on catchability (q) resulted in a posterior (maximum likelihood Bayesian $q_N = 3.870 \times 10^{-3}$; Figure 5, left, and Equation A9-N) that was closer to the pre-season prior (prior $q_N = 3.681 \times 10^{-3}$; Figure 5, left, and Equation A4-N) than to the in-season depletion (depletion $q_N = 5.460 \times 10^{-3}$; Figure 5, left, and A6-N). Respective weights in the Bayesian optimization (converse of the CVs) were 0.493 for the in-season depletion (A5-N) and 0.298 for the prior (A8-N).

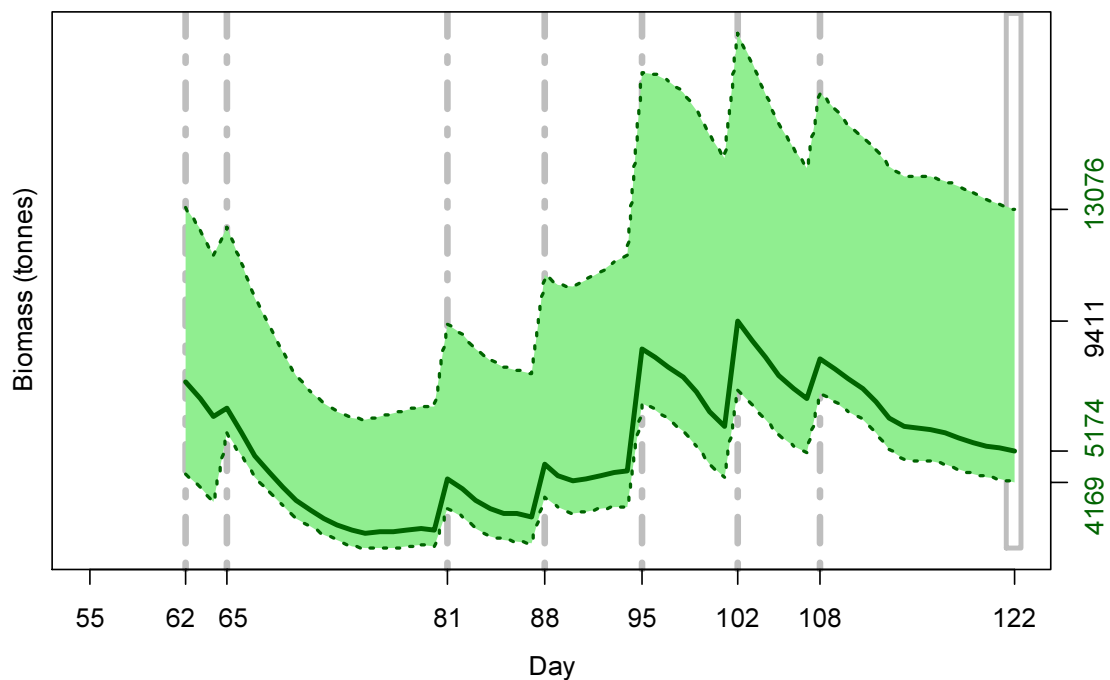
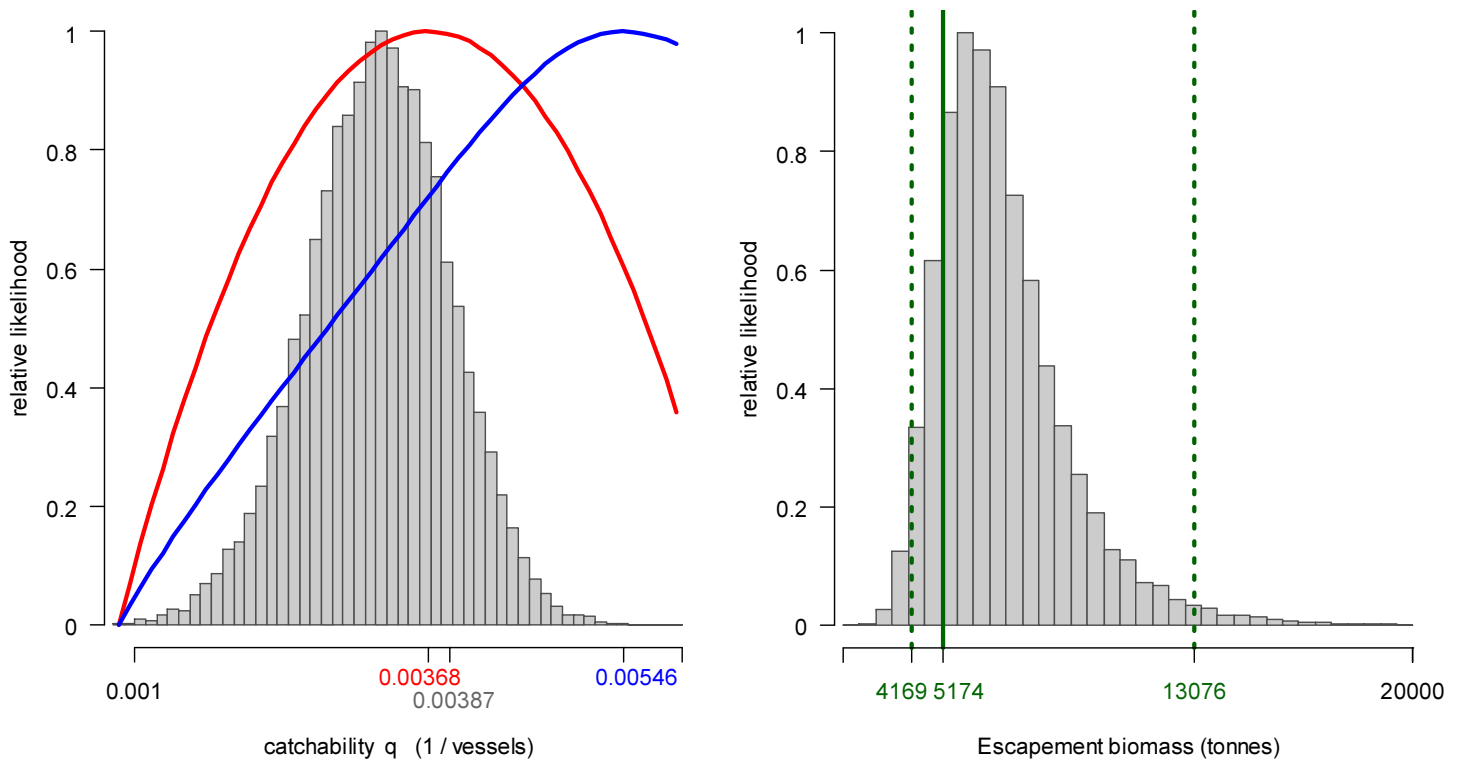


Figure 5 [previous page, upper]. North sub-area. Left: Likelihood distributions for calamari catchability. Red line: prior model (pre-season survey data), blue line: in-season depletion model, grey bars: combined Bayesian model. Right: Likelihood distribution (grey bars) of escapement biomass, from Bayesian posterior and average individual calamari weight at the end of the season. Green lines: maximum likelihood and 95% confidence interval. Note correspondence to Figure 6.

Figure 6 [previous page, lower]. North sub-area. Calamari biomass time series estimated from Bayesian posterior of the depletion model \pm 95% confidence intervals. Broken grey bars indicate the start of in-season depletions north; days 62, 65, 81, 88, 95, 102 and 108. Note that the biomass ‘footprint’ on day 122 (May 1st) corresponds to the right-side plot of Figure 5.

The MCMC distribution of the Bayesian posterior multiplied by the GAM fit of average individual calamari weight (Figure A1-north) gave the likelihood distribution of calamari biomass on day 122 (May 1st) shown in Figure 5-right, with maximum likelihood and 95% confidence interval of:

$$B_{N \text{ day } 122} = 5,174 \text{ t} \sim 95\% \text{ CI } [4,169 - 13,076] \text{ t} \quad (8)$$

At its highest point (penultimate depletion start: day 102 – April 11th), estimated calamari biomass north was 9,411 t \sim 95% CI [7,176 – 18,867] t (Figure 6).

South

In the south sub-area, relative ranks of catchability coefficients (q) were reversed from the north as the pre-season prior $q_S = 1.156 \times 10^{-3}$ (Figure 7 left, and equation **A4-S**) was higher than the Bayesian posterior maximum likelihood $q_S = 1.136 \times 10^{-3}$ (Figure 7, left, and equation **A9-S**), while the in-season depletion was lower $q_S = 0.824 \times 10^{-3}$ (Figure 7, left, and **A6-S**). Bayesian optimization was weighted 0.496 for in-season depletion (**A5-S**) vs. 0.235 for the prior (**A8-S**).

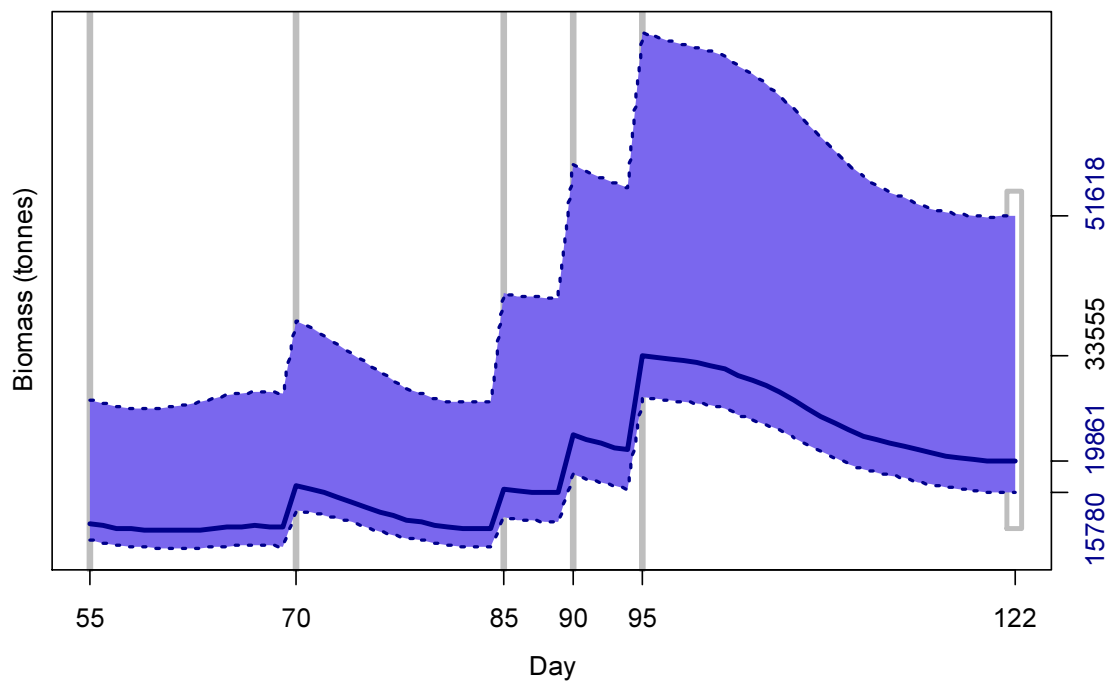
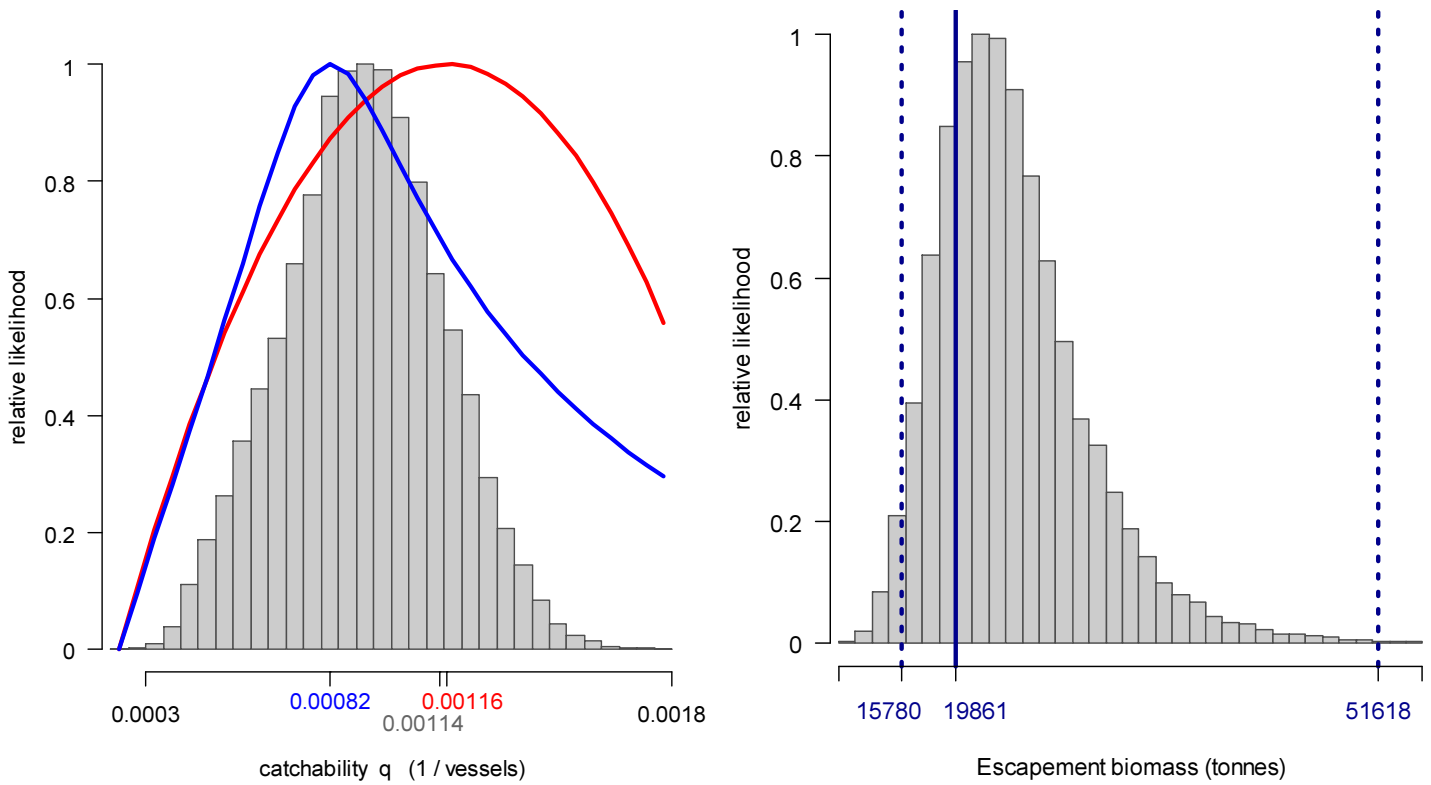
The MCMC distribution of the Bayesian posterior multiplied by the GAM fit of average individual calamari weight (Figure A1-south) gave the likelihood distribution of calamari biomass on day 122 (May 1st) shown in Figure 7-right, with maximum likelihood and 95% confidence interval of:

$$B_{S \text{ day } 122} = 19,861 \text{ t} \sim 95\% \text{ CI } [15,780 - 51,618] \text{ t} \quad (9)$$

At its highest point (last depletion start day 95; April 4th), estimated calamari biomass south was 33,555 t \sim 95% CI [28,156 – 75,568] t (Figure 8).

Figure 7 [next page]. South sub-area. Left: Likelihood distributions for calamari catchability. Red line: prior model (pre-season survey data), blue line: in-season depletion model, grey bars: combined Bayesian model. Right: Likelihood distribution (grey bars) of escapement biomass, from Bayesian posterior and average individual calamari weight at the end of the season. Blue lines: max. likelihood and 95% conf. interval. Note correspondence to Fig. 8.

Figure 8 [next page, lower]. South sub-area. Calamari biomass time series estimated from Bayesian posterior of the depletion model \pm 95% confidence intervals. Gray bars indicate the start of in-season depletions south; days 55, 70, 85, 90 and 95. Note that the biomass ‘footprint’ on day 122 (May 1st) corresponds to the right-side plot of Figure 7.



Escapement biomass

Total escapement biomass was defined as the aggregate biomass of Falkland calamari at the end of day 122 (May 1st) for north and south sub-areas combined (equations 8 and 9). Depletion models are calculated on the inference that all fishing and natural mortality are gathered at mid-day, thus a half day of mortality ($e^{-M/2}$) was added to correspond to the closure of the fishery at 23:59 (mid-night) on May 1st for the final

remaining vessel: equation 10. Semi-randomized addition of the north and south biomass estimates gave the aggregate likelihood distribution of total escapement biomass shown in Figure 9.

$$\begin{aligned}
 B_{\text{Total day 122}} &= (B_{\text{N day 122}} + B_{\text{S day 122}}) \times e^{-M/2} \\
 &= 24,868 \text{ t} \sim 95\% \text{ CI } [20,723 - 61,272] \text{ t}
 \end{aligned}
 \tag{10}$$

This escapement biomass gave the uncommon result that a greater abundance of calamari was present at the end of the season than at the beginning of the season (21,729 t; Winter et al., 2016). Among both 1st and 2nd seasons since 2010, only in 1st season 2013 was a similar contrast obtained, when the pre-season survey biomass was estimated at a very low 5333 tonnes (Winter et al., 2013). Notably, the current pre-season survey biomass estimate of 21,729 t is the lowest since 1st season 2013.

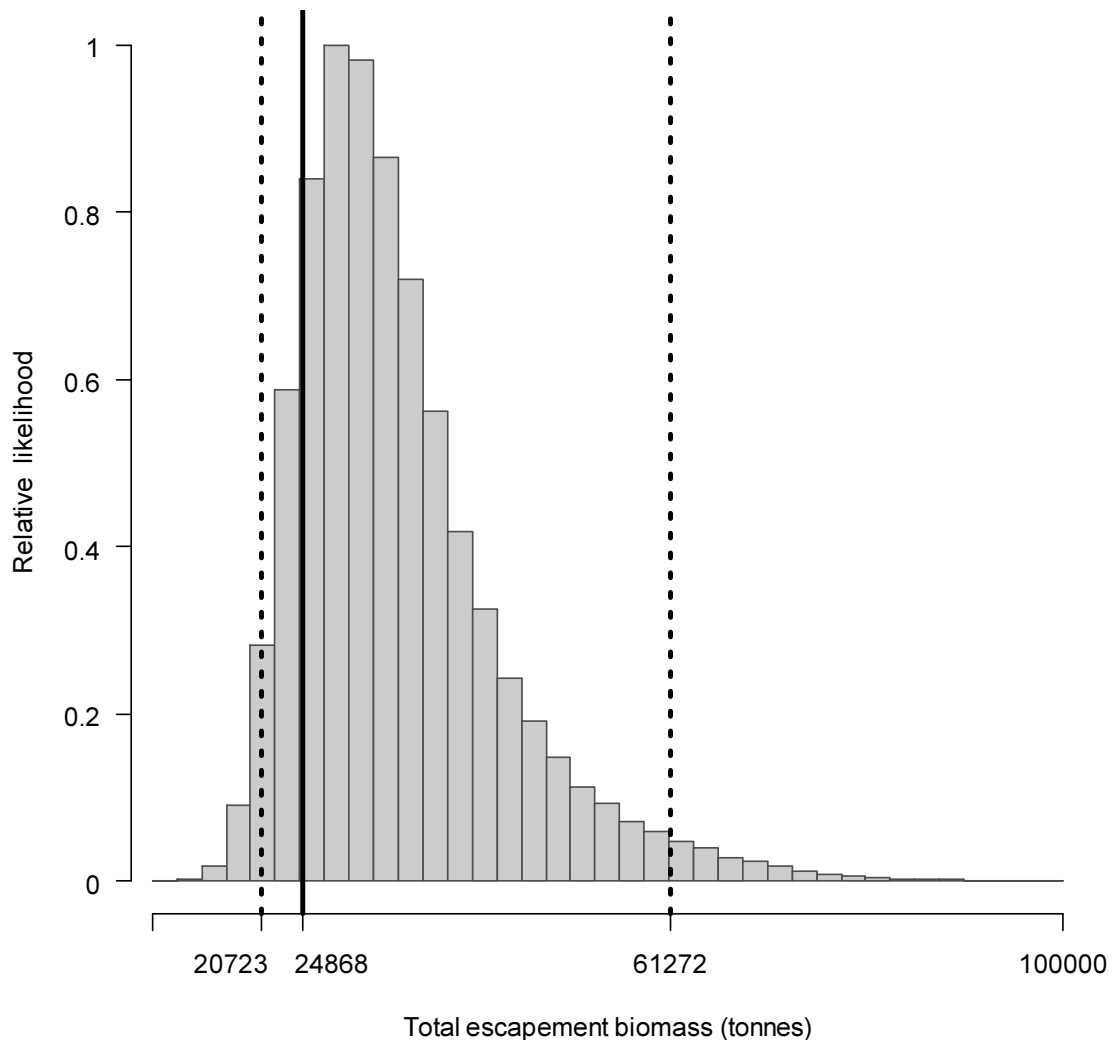


Figure 9. Likelihood distribution with 95% confidence intervals of total Falkland calamari escapement biomass corresponding to the season end (May 1st).

The risk of the fishery in the current season, defined as the proportion of the total escapement biomass distribution below the conservation limit of 10,000 tonnes (Agnew et al., 2002; Barton, 2002), was calculated as effectively zero.

Immigration

Falkland calamari immigration during the season was inferred on each day by how many more calamari were estimated present than the day before, minus the number caught and the number expected to have died naturally:

$$\text{Immigration } N_{\text{day } i} = N_{\text{day } i} - (N_{\text{day } i-1} - C_{\text{day } i-1} - M_{\text{day } i-1})$$

where $N_{\text{day } i-1}$ are optimized in the depletion models, $C_{\text{day } i-1}$ calculated as in equation 2, and $M_{\text{day } i-1}$ is:

$$M_{\text{day } i-1} = (N_{\text{day } i-1} - C_{\text{day } i-1}) \times (1 - e^{-M})$$

Immigration biomass per day was then calculated as the immigration number per day multiplied by predicted average individual weight from the GAM:

$$\text{Immigration } B_{\text{day } i} = \text{Immigration } N_{\text{day } i} \times \text{GAM } W_{\text{day } i}$$

All numbers N are themselves derived from the daily average individual weights, so the estimation factors in that those calamari immigrating on a day would likely be smaller than average. Confidence intervals of the immigration estimates were calculated by applying the above algorithms to the MCMC iterations of the depletion models. Resulting total biomasses of calamari immigration north and south, up to season end (day 122), were:

$$\text{Immigration } B_{N \text{ day } 62-122} = 13,290 \text{ t} \sim 95\% \text{ CI } [11,906 - 22,803] \text{ t} \quad \text{(11-N)}$$

$$\text{Immigration } B_{S \text{ day } 55-122} = 30,584 \text{ t} \sim 95\% \text{ CI } [25,402 - 63,055] \text{ t} \quad \text{(11-S)}$$

Total immigration with semi-randomized addition of the confidence intervals was:

$$\text{Immigration } B_{\text{Total } 55-111} = 43,874 \text{ t} \sim 95\% \text{ CI } [38,489 - 82,768] \text{ t} \quad \text{(11-T)}$$

In the north sub-area, the in-season peaks on days 65, 81, 88, 95, 102 and 108 accounted for 4.7%, 7.4%, 8.1%, 16.8%, 15.4% and 6.9% of in-season immigration (start day 55 was de facto not an in-season immigration), consistent with the variation in the time series biomass shown on Figure 6. In the south sub-area, the in-season peaks on days 70, 85, 90 and 95 accounted for 13.5%, 12.8%, 18.9% and 30.6% of in-season immigration, consistent with the variation in the time series biomass shown on Figure 8.

Size ranges

Concurrent with the bulk of calamari biomass having entered the fishing zone only late in the season, calamari catch individual size distributions during the 2016 1st

season were small compared to previous 1st seasons. The median mantle length of both male and female calamari, north and south of 52°S, was 9.5 - 10 cm in the 2016 1st season. In the 2013 1st season, median mantle lengths south were similar at 9.5 - 10 cm, but bigger north at 11.5 cm. No other 1st seasons since at least 2009 had size distributions this small (Figure 10).

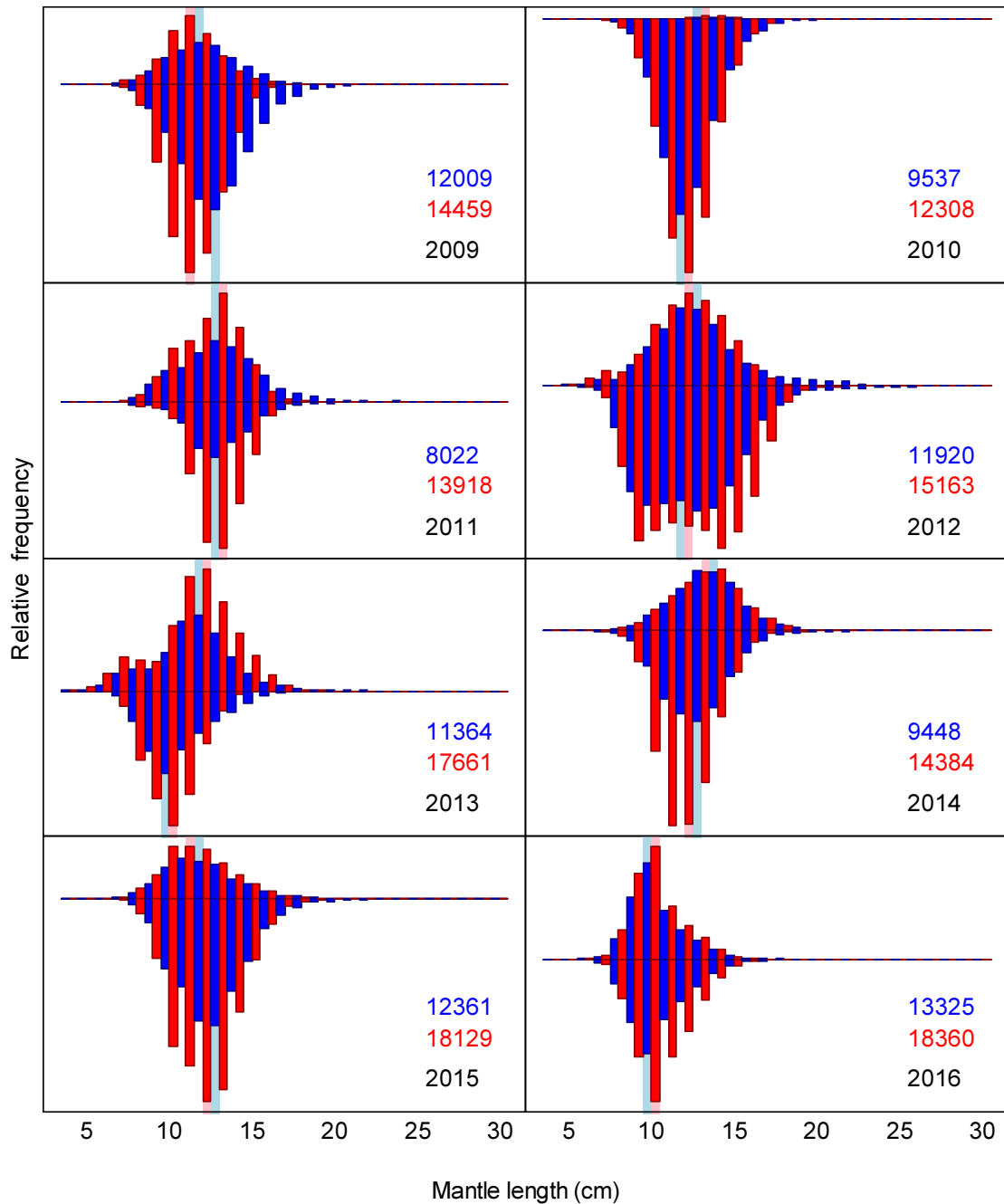
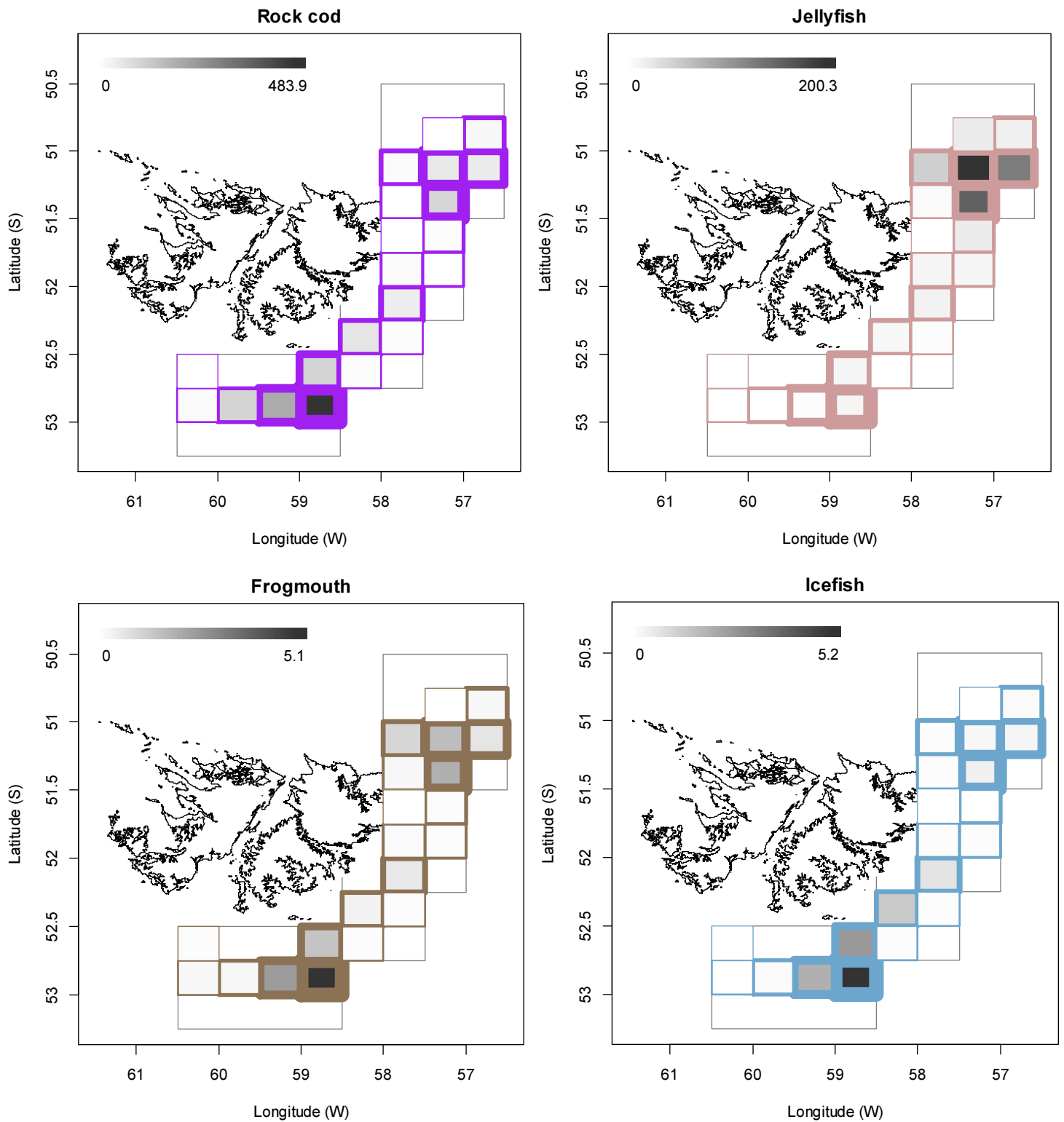
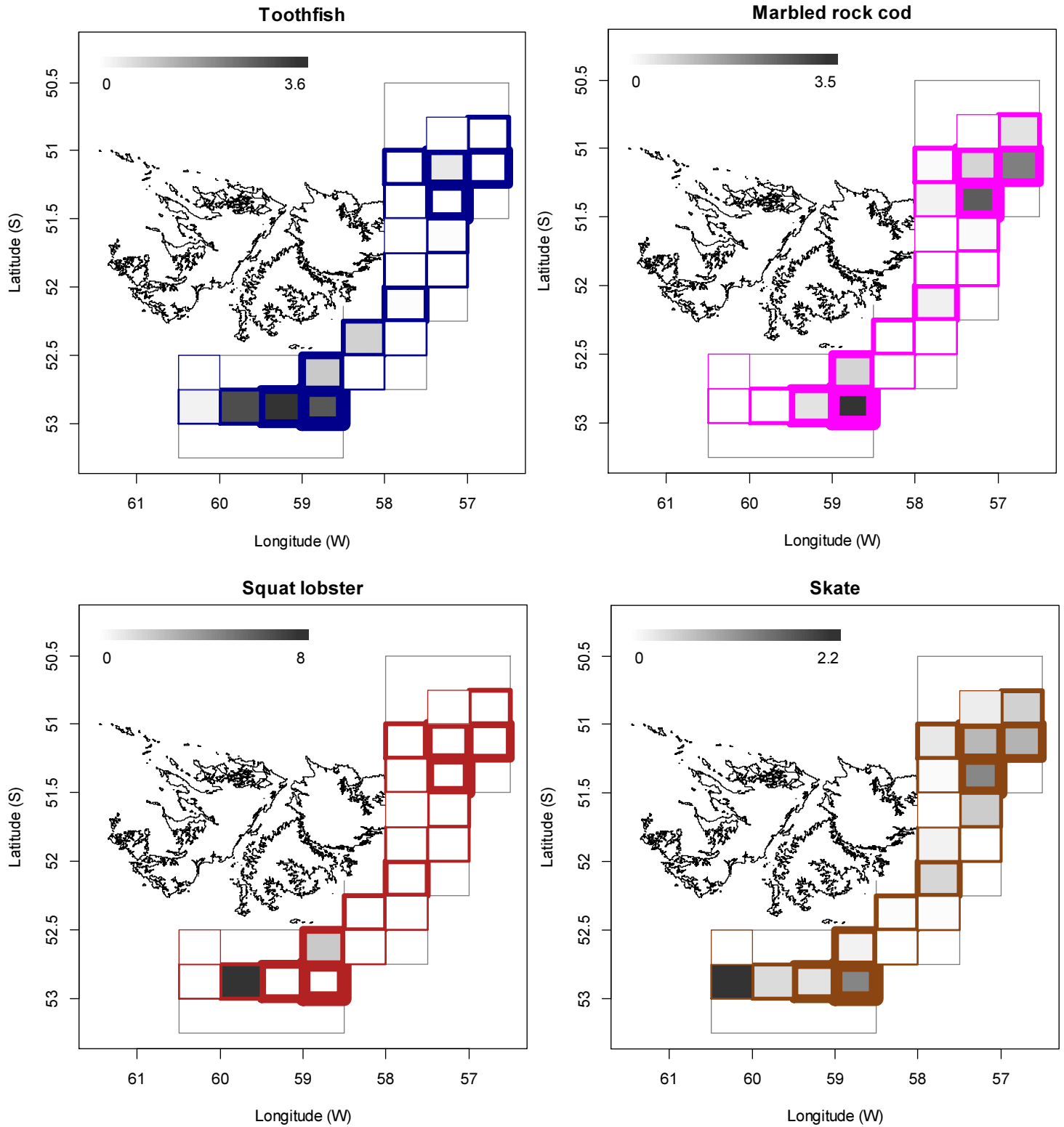


Figure 10. Falkland calamari mantle-length distributions from in-season observer random samples, 1st seasons 2009 – 2016. Distributions are partitioned north (up) and south (down) of latitude 52°S, males (blue) and females (red). Median lengths in light blue and pink are underlaid on the plots. Numbers of male and female calamari sampled each season are noted on each plot.

Bycatch

Figure 11 [below]. Distributions of the eight principal bycatches during 1st calamari season 2016. Thickness of grid lines is proportional to the number of vessel-days (1 to 242). Gray-scale is proportional to the bycatch biomass; maximum (tonnes) indicated on each plot.





Of the 1020 calamari-target vessel-days in total (Table 1), only 3 vessel-days reported a primary catch other than calamari, which were 50.2%, 50.7%, and 54.4% rock cod (*Patagonotothen ramsayi*). The most common bycatches reported overall for the Falkland calamari season were rock cod (1296 t, reported from 969 vessel-days), jellyfish (Medusae) (654 t, 540 vessel-days), frogmouth (*Cottoperca gobio*) (17 t, 296

vessel-days), icefish (*Champsocephalus esox*) (13 t, 285 vessel-days), Patagonian toothfish (*Dissostichus eleginoides*) (12 t, 116 vessel-days), marbled rock cod (*Patagonotothen tessellata*) (12 t, 86 vessel-days), squat lobster (*Munida* spp.) (10 t, 9 vessel-days) and skate (Rajidae) (10 t, 167 vessel-days). Relative distributions by grid of these bycatches are shown in Figure 11.

References

- Agnew, D.J., Baranowski, R., Beddington, J.R., des Clers, S., Nolan, C.P. 1998. Approaches to assessing stocks of *Loligo gahi* around the Falkland Islands. Fisheries Research 35: 155-169.
- Agnew, D. J., Beddington, J. R., and Hill, S. 2002. The potential use of environmental information to manage squid stocks. Canadian Journal of Fisheries and Aquatic Sciences, 59: 1851–1857.
- Arkhipkin, A.I., Middleton, D.A.J. 2002. Sexual segregation in ontogenetic migrations by the squid *Loligo gahi* around the Falkland Islands. Bulletin of Marine Science 71: 109-127.
- Arkhipkin, A.I., Middleton, D.A.J., Barton, J. 2008. Management and conservation of a short-lived fishery resource: *Loligo gahi* around the Falkland Islands. American Fisheries Society Symposium 49: 1243-1252.
- Barton, J. 2002. Fisheries and fisheries management in Falkland Islands Conservation Zones. Aquatic Conservation: Marine and Freshwater Ecosystems 12: 127–135.
- Bradley, K. 2016a. Observer Report 1087. Technical Document, FIG Fisheries Department. 23 p.
- Bradley, K. 2016b. Observer Report 1097. Technical Document, FIG Fisheries Department. 32 p.
- Brooks, S.P., Gelman, A. 1998. General methods for monitoring convergence of iterative simulations. Journal of computational and graphical statistics 7:434-455.
- DeLury, D.B. 1947. On the estimation of biological populations. Biometrics 3: 145-167.
- Gamerman, D., Lopes, H.F. 2006. Markov Chain Monte Carlo. Stochastic simulation for Bayesian inference. 2nd edition. Chapman & Hall/CRC.
- Iriarte, V. 2016. Observer Report 1090. Technical Document, FIG Fisheries Department. 27 p.
- Magnusson, A., Punt, A., Hilborn, R. 2013. Measuring uncertainty in fisheries stock assessment: the delta method, bootstrap, and MCMC. Fish and Fisheries 14: 325-342.
- Nash, J.C., Varadhan, R. 2011. optimx: A replacement and extension of the optim() function. R package version 2011-2.27. <http://CRAN.R-project.org/package=optimx>
- Patterson, K.R. 1988. Life history of Patagonian squid *Loligo gahi* and growth parameter estimates using least-squares fits to linear and von Bertalanffy models. Marine Ecology Progress Series 47: 65-74.

- Payá, I. 2009. Fishery Report. *Loligo gahi*, First Season 2009. Fishery statistics, biological trends, stock assessment and risk analysis. Technical Document, Falkland Islands Fisheries Department. 41 p.
- Payá, I. 2010. Fishery Report. *Loligo gahi*, Second Season 2009. Fishery statistics, biological trends, stock assessment and risk analysis. Technical Document, Falkland Islands Fisheries Department. 54 p.
- Punt, A.E., Hilborn, R. 1997. Fisheries stock assessment and decision analysis: the Bayesian approach. *Reviews in Fish Biology and Fisheries* 7:35-63.
- Roa-Ureta, R. 2012. Modelling in-season pulses of recruitment and hyperstability-hyperdepletion in the *Loligo gahi* fishery around the Falkland Islands with generalized depletion models. *ICES Journal of Marine Science* 69: 1403–1415.
- Roa-Ureta, R., Arkhipkin, A.I. 2007. Short-term stock assessment of *Loligo gahi* at the Falkland Islands: sequential use of stochastic biomass projection and stock depletion models. *ICES Journal of Marine Science* 64: 3-17.
- Rosenberg, A.A., Kirkwood, G.P., Crombie, J.A., Beddington, J.R. 1990. The assessment of stocks of annual squid species. *Fisheries Research* 8: 335-350.
- Shaw, P.W., Arkhipkin, A.I., Adcock, G.J., Burnett, W.J., Carvalho, G.R., Scherbich, J.N., Villegas, P.A. 2004. DNA markers indicate that distinct spawning cohorts and aggregations of Patagonian squid, *Loligo gahi*, do not represent genetically discrete subpopulations. *Marine Biology*, 144: 961-970.
- Winter, A. 2011. *Loligo gahi* stock assessment, first season 2011. Technical Document, Falkland Islands Fisheries Department. 23 p.
- Winter, A. 2012. *Loligo gahi* stock assessment, first season 2012. Technical Document, Falkland Islands Fisheries Department. 27 p.
- Winter, A. 2013. *Loligo* stock assessment, first season 2013. Technical Document, Falkland Islands Fisheries Department. 23 p.
- Winter, A. 2014a. *Loligo* stock assessment, first season 2014. Technical Document, Falkland Islands Fisheries Department. 28 p.
- Winter, A. 2014b. *Loligo* stock assessment, second season 2014. Technical Document, Falkland Islands Fisheries Department. 30 p.
- Winter, A., Arkhipkin, A. 2015. Environmental impacts on recruitment migrations of Patagonian longfin squid (*Doryteuthis gahi*) in the Falkland Islands with reference to stock assessment. *Fisheries Research* 172: 85-95.
- Winter, A., Jürgens, L., Monllor, A. 2013. *Loligo* stock assessment survey, 1st season 2013. Technical Document, Falkland Islands Fisheries Department. 15 p.
- Winter, A., Zawadowski, T., Shcherbich, Z., Bradley, K., Kuepfer, A. 2016. Falkland calamari stock assessment survey, 1st season 2016. Technical Document, Falkland Islands Fisheries Department. 19 p.

Appendix

Falkland calamari individual weights

A generalized additive model (GAM) was calculated from the daily observer data (both sexes combined) and commercial size category data of average individual daily weights of calamari. North and south sub-areas were calculated separately. For continuity, the GAMs were calculated using all pre-season survey and in-season data contiguously. GAM plots of the north and south sub-areas are shown in Figure A1.

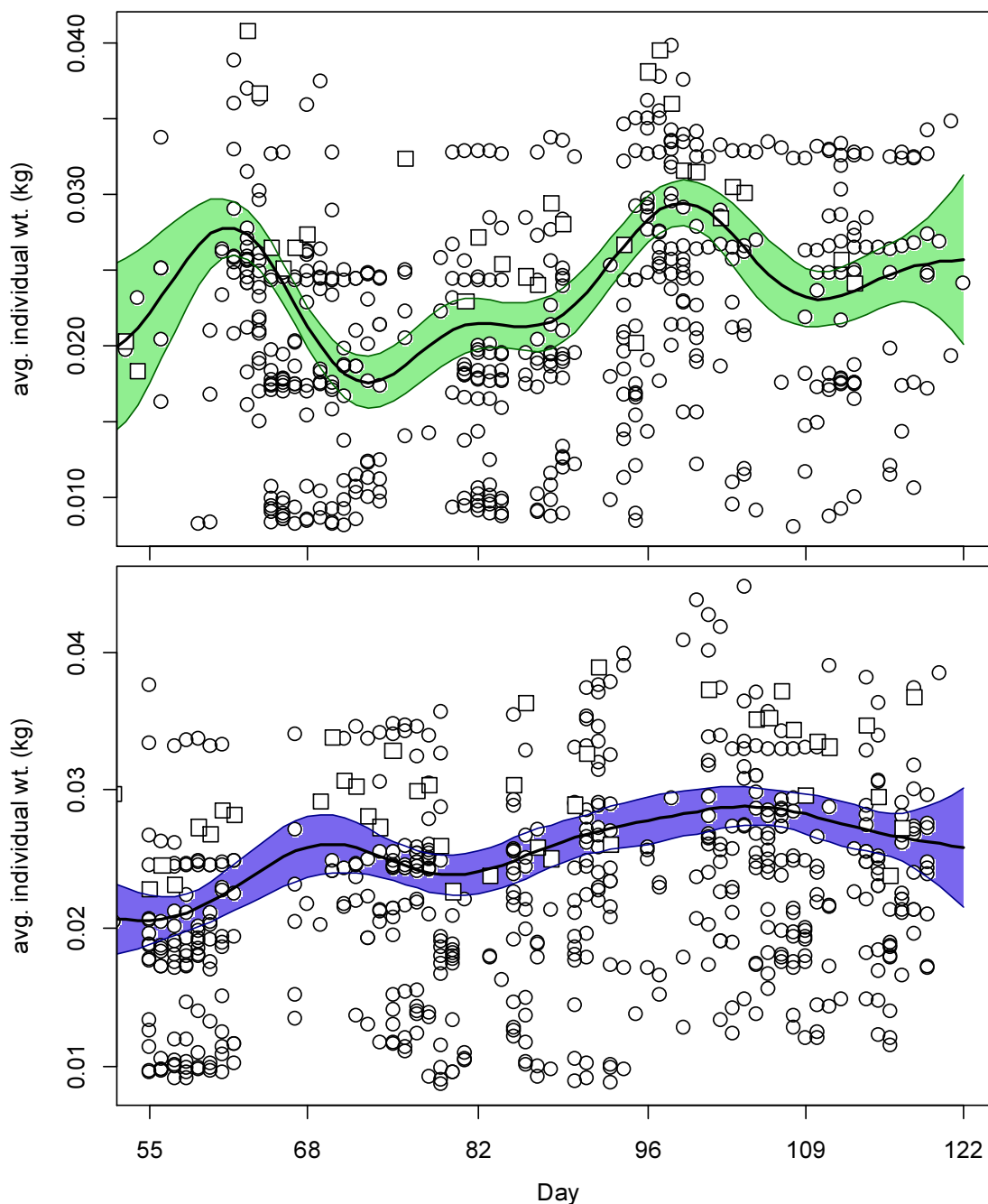


Figure A1. North (top) and south (bottom) sub-area daily average individual calamari weights from commercial size categories per vessel (circles) and observer measurements (squares). GAMs of the daily trends \pm 95% confidence intervals (centre lines and colour under-shading).

Prior estimates and CV

The pre-season survey (Winter et al., 2016) had estimated Falkland calamari biomasses of 8,520 t (standard deviation: $\pm 1,404$ t) north of 52° S and 13,209 t (standard deviation: 1,767 t) south of 52° S. From modelled survey catchability, Payá (2010) had estimated average net escapement of up to 22%, which was added to the standard deviation:

$$8,520 \pm \left(\frac{1,404}{8,520} + .22 \right) = 8,520 \pm 38.5\% = 8,520 \pm 3,278 \text{ t} \quad (\text{A1-N})$$

$$13,209 \pm \left(\frac{1,767}{13,209} + .22 \right) = 13,209 \pm 35.4\% = 13,209 \pm 4,673 \text{ t} \quad (\text{A1-S})$$

The 22% was added as a linear increase in the variability, but was not used to reduce the total estimate, because calamari that escape one trawl are likely to be part of the biomass concentration that is available to the next trawl.

Calamari numbers at the start of the season, day 55, were estimated as the survey biomasses divided by the GAM-predicted individual weight averages for the survey: 0.022 kg north and 0.021 kg south (Figure A1). Average coefficients of variation (CV) of the GAM over the duration of the pre-season survey were 12.69% north and 8.46% south, and CV of the length-weight conversion relationship (equation 8) were 6.6% north and 6.9% south. Combining all sources of variation with the pre-season survey biomass estimates and average individual weight averages gave estimated calamari numbers at season start (February 24th; day 55) of:

$$\begin{aligned} \text{prior } N_{N \text{ day } 55} &= \frac{8,520 \times 1000}{0.022} \pm \sqrt{38.5\%^2 + 12.69\%^2 + 6.6\%^2} \\ &= 0.384 \times 10^9 \pm 41.1\% \end{aligned} \quad (\text{A2-N})$$

$$\begin{aligned} \text{prior } N_{S \text{ day } 55} &= \frac{13,209 \times 1000}{0.021} \pm \sqrt{35.4\%^2 + 8.46\%^2 + 6.9\%^2} \\ &= 0.645 \times 10^9 \pm 37.0\% \end{aligned} \quad (\text{A2-S})$$

The catchability coefficient (q) prior for the north sub-area was taken on day 62, when 9 vessels were fishing north and the 1st depletion period north started. The abundance prior (N) on day 62 was calculated as survey abundance on start day 55 discounted for 7 days of natural mortality (as no catch had been taken in those 2 days):

$$\text{prior } N_{N \text{ day } 62} = \text{prior } N_{N \text{ day } 55} \times e^{-M \cdot (62 - 55)} - \text{CNMD}_{\text{day } 62} = 0.347 \times 10^9 \quad (\text{A3-N})$$

$$\begin{aligned} \text{prior } q_N &= C(N)_{N \text{ day } 62} / (\text{prior } N_{N \text{ day } 62} \times E_{N \text{ day } 62}) \\ &= (C(B)_{N \text{ day } 62} / W_{t_{N \text{ day } 62}}) / (\text{prior } N_{N \text{ day } 62} \times E_{N \text{ day } 62}) \\ &= (318.9 \text{ t} / 0.028 \text{ kg}) / (0.347 \times 10^9 \times 9 \text{ vessel-days}) \end{aligned}$$

$$= 3.681 \times 10^{-3} \text{ vessels}^{-1} \text{ }^A \quad (\text{A4-N})$$

The catchability coefficient (q) prior for the south sub-area was taken on day 55, when all 16 vessels were fishing south. As this was the first scheduled day of the season, no discount was applicable for either natural mortality or catch.

$$\begin{aligned} \text{prior } q_S &= C(N)_{S \text{ day } 55} / (\text{prior } N_{S \text{ day } 55} \times E_{S \text{ day } 55}) \\ &= (C(B)_{S \text{ day } 55} / Wt_{S \text{ day } 55}) / (\text{prior } N_{S \text{ day } 55} \times E_{S \text{ day } 55}) \\ &= (245.7 \text{ t} / 0.021 \text{ kg}) / (0.645 \times 10^9 \times 16 \text{ vessel-days}) \\ &= 1.156 \times 10^{-3} \text{ vessels}^{-1} \text{ }^B \end{aligned} \quad (\text{A4-S})$$

CVs of the priors were calculated as the sums of variability in $\text{prior } N$ (equations A2) plus variability in the catches of vessels on the start days (day 62 N and day 55 S):

$$\begin{aligned} CV_{\text{prior } N} &= \sqrt{41.1\%^2 + \left(\frac{SD(C(B)_{N \text{ vessels day } 62})}{\text{mean}(C(B)_{N \text{ vessels day } 62})} \right)^2} \\ &= \sqrt{41.1\%^2 + 27.3\%^2} = 49.3\% \end{aligned} \quad (\text{A5-N})$$

$$\begin{aligned} CV_{\text{prior } S} &= \sqrt{37.0\%^2 + \left(\frac{SD(C(B)_{S \text{ vessels day } 55})}{\text{mean}(C(B)_{S \text{ vessels day } 55})} \right)^2} \\ &= \sqrt{37.0\%^2 + 33.0\%^2} = 49.6\% \end{aligned} \quad (\text{A5-S})$$

Depletion model estimates and CV

For the north sub-area, the equivalent of equation 2 with seven N_{day} was optimized on the difference between predicted catches and actual catches (equation 3), resulting in parameters values:

$$\begin{aligned} \text{depletion } N1_{N \text{ day } 62} &= 0.191 \times 10^9; & \text{depletion } N2_{N \text{ day } 65} &= 0.057 \times 10^9 \\ \text{depletion } N3_{N \text{ day } 81} &= 0.074 \times 10^9; & \text{depletion } N4_{N \text{ day } 88} &= 0.077 \times 10^9 \\ \text{depletion } N5_{N \text{ day } 95} &= 0.127 \times 10^9; & \text{depletion } N6_{N \text{ day } 102} &= 0.111 \times 10^9 \\ \text{depletion } N7_{N \text{ day } 108} &= 0.073 \times 10^9 \\ \text{depletion } q_N &= 5.460 \times 10^{-3} \text{ }^C \end{aligned} \quad (\text{A6-N})$$

The root-mean-square deviation of predicted vs. actual catches was calculated as the CV of the model:

^A On Figure 5-left.

^B On Figure 7-left.

^C On Figure 5-left.

$$\begin{aligned}
CV_{\text{rmsd N}} &= \frac{\sqrt{\sum_{i=1}^n \left(\text{predicted } C(N)_{\text{N day } i} - \text{actual } C(N)_{\text{N day } i} \right)^2 / n}}{\text{mean}(\text{actual } C(N)_{\text{N day } i})} \\
&= 2.395 \times 10^6 / 8.107 \times 10^6 = 29.5\% \quad (\text{A7-N})
\end{aligned}$$

$CV_{\text{rmsd N}}$ was added to the variability of the GAM-predicted individual weight averages for the season (Figure A1-N); equal to a CV of 4.0% north. CVs of the depletion were then calculated as the sum:

$$\begin{aligned}
CV_{\text{depletion N}} &= \sqrt{CV_{\text{rmsd N}}^2 + CV_{\text{GAM Wt N}}^2} = \sqrt{29.5\%^2 + 4.0\%^2} \\
&= 29.8\% \quad (\text{A8-N})
\end{aligned}$$

For the south sub-area, the equivalent of equation 2 with five N_{day} was optimized on the difference between predicted catches and actual catches (equation 3), resulting in parameters values:

$$\begin{aligned}
\text{depletion N1}_{\text{S day 55}} &= 0.767 \times 10^9; & \text{depletion N2}_{\text{S day 70}} &= 0.260 \times 10^9 \\
\text{depletion N3}_{\text{S day 85}} &= 0.268 \times 10^9; & \text{depletion N4}_{\text{S day 90}} &= 0.391 \times 10^9 \\
\text{depletion N5}_{\text{S day 95}} &= 0.566 \times 10^9 \\
\text{depletion Q S} &= 0.824 \times 10^{-3 \text{ D}} \quad (\text{A6-S})
\end{aligned}$$

The normalized root-mean-square deviation of predicted vs. actual catches was calculated as the CV of the model:

$$\begin{aligned}
CV_{\text{rmsd S}} &= \frac{\sqrt{\sum_{i=1}^n \left(\text{predicted } C(N)_{\text{S day } i} - \text{actual } C(N)_{\text{S day } i} \right)^2 / n}}{\text{mean}(\text{actual } C(N)_{\text{S day } i})} \\
&= 1.673 \times 10^6 / 7.179 \times 10^6 = 23.3\% \quad (\text{A7-S})
\end{aligned}$$

$CV_{\text{rmsd S}}$ was added to the variability of the GAM-predicted individual weight averages for the season (Figure A1-S); equal to a CV of 3.2% south. CVs of the depletion were then calculated as the sum:

$$\begin{aligned}
CV_{\text{depletion S}} &= \sqrt{CV_{\text{rmsd S}}^2 + CV_{\text{GAM Wt S}}^2} = \sqrt{23.3\%^2 + 3.2\%^2} \\
&= 23.5\% \quad (\text{A8-S})
\end{aligned}$$

Combined Bayesian models

For the north sub-area, the joint optimization of equations 3 and 4 resulted in parameters values:

^D On Figure 7-left.

Bayesian N_{1N} day 62	= 0.268×10^9 ;	Bayesian N_{2N} day 65	= 0.036×10^9
Bayesian N_{3N} day 81	= 0.082×10^9 ;	Bayesian N_{4N} day 88	= 0.089×10^9
Bayesian N_{5N} day 95	= 0.152×10^9 ;	Bayesian N_{6N} day 102	= 0.133×10^9
Bayesian N_{7N} day 108	= 0.067×10^9		
Bayesian Q_N	= 3.870×10^{-3} ^E		(A9-N)

These parameters produced the fit between predicted and actual catches shown in Figure A2-N.

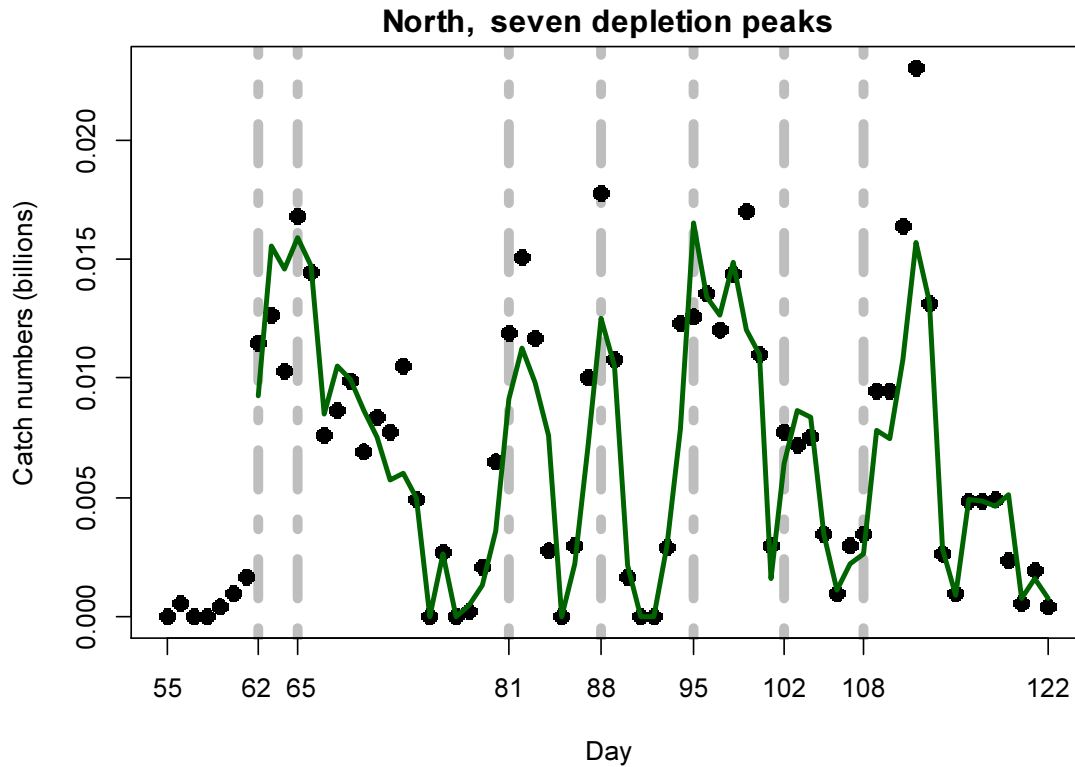


Figure A2-N. Daily catch numbers estimated from actual catch (black points) and predicted from the depletion model (green line) in the north sub-area.

For the south sub-area, the joint optimization of equations 3 and 4 resulted in parameters values:

Bayesian N_{1S} day 55	= 0.568×10^9 ;	Bayesian N_{2S} day 70	= 0.204×10^9
Bayesian N_{3S} day 85	= 0.207×10^9 ;	Bayesian N_{4S} day 90	= 0.292×10^9
Bayesian N_{3S} day 95	= 0.458×10^9		
Bayesian Q_S	= 1.136×10^{-3} ^F		(A9-S)

These parameters produced the fit between predicted and actual catches shown in Figure A2-S.

^E On Figure 5-left.

^F On Figure 7-left.

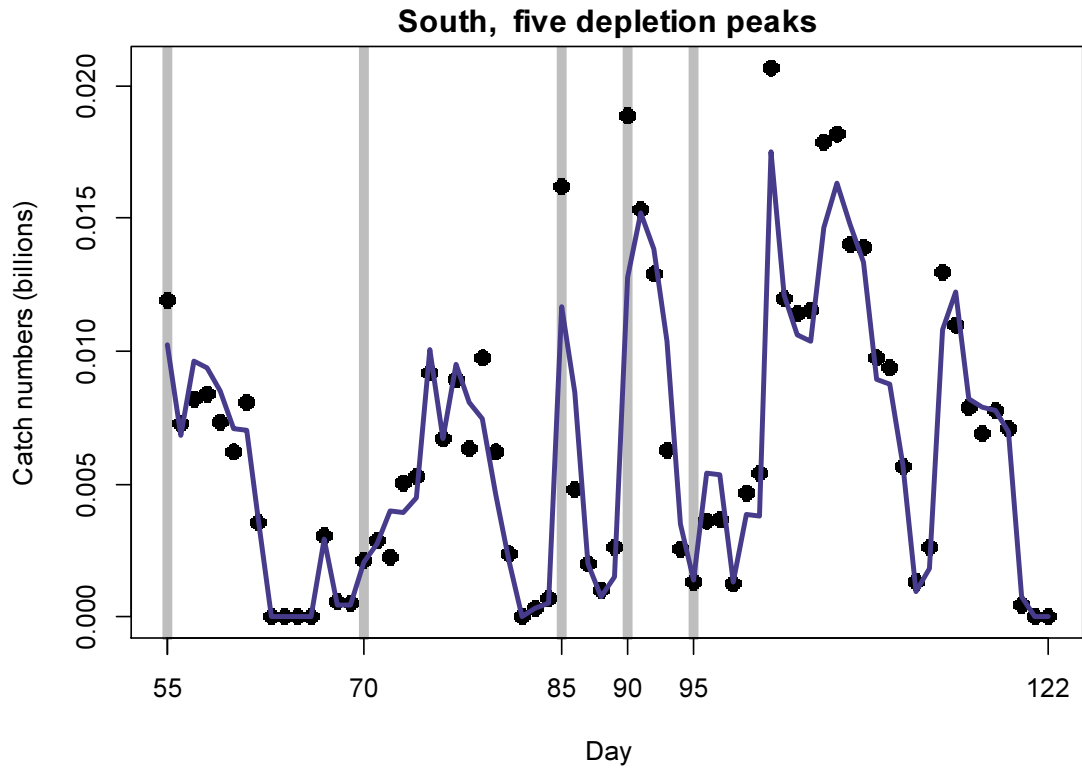


Figure A2-S. Daily catch numbers estimated from actual catch (black points) and predicted from the depletion model (blue line) in the south sub-area.